



Bis(1,3-dithiole-2-one-4,5-dithiolato)antimonate(1-) salts, [Q][Sb(dmio)₂]. Structural comparisons of [Q][Sb(dmio)₂] and bis(1,3-dithiole-2-thione-4,5-dithiolato)antimonate(1-) salts, [Q][Sb(dmit)₂]

John H. Aupers^a, Zahid H. Chohan^b, Nadia M. Comerlato^c, R. Alan Howie^{a,*},
Alexandre C. Silvino^c, James L. Wardell^c, Solange M.S.V. Wardell^d

^a Department of Chemistry, University of Aberdeen, Meston Walk, Old Aberdeen AB24 3UE, UK

^b Department of Chemistry, Islamia University, Bahawalpur, Pakistan

^c Departamento de Química Inorgânica, Instituto de Química, Universidade Federal do Rio de Janeiro, CP 68563, 21945-970 Rio de Janeiro, RJ, Brazil

^d Departamento de Química Orgânica, Instituto de Química, Universidade Federal Fluminense, 24020-150 Niterói, RJ, Brazil

Received 19 March 2002; accepted 12 June 2002

Abstract

Bis(1,3-dithiole-2-one-4,5-dithiolato)antimonate(1-) salts, [Q][Sb(C₃OS₄)₂], [Q][Sb(dmio)₂] (3: Q = NEt₄, 1,4-dimethylpyridinium (DMP), PPh₄ or ferrocenyl-CH₂NMe₃) and bis(1,3-dithiole-2-thione-4,5-dithiolato)antimonate(1-) salts, [Q][Sb(C₃S₅)₂], [Q][Sb(dmit)₂] (1: Q = AsPh₄ or NBu₄) have been obtained from SbBr₃–NaSCN and [Q]₂[Zn(dmio)₂] or [Q]₂[Zn(dmit)₂]. The crystal structures of (1: Q = AsPh₄ or NBu₄) and (3: Q = NEt₄ and DMP) have been determined. In all cases, the Sb centres are 6-coordinated and, with the inclusion of the lone pair, are considered to have pseudo pentagonal bipyramidal structures. The interanion interactions in these and related complexes are compared.

© 2002 Elsevier Science Ltd. All rights reserved.

Keywords: 1,3-Dithiole-2-thione-4,5-dithiolates; 1,3-Dithiole-2-one-4,5-dithiolates; Antimony(III); Crystal structures

1. Introduction

The 1,3-dithiole-2-thione-4,5-dithiolate dianion, [C₃S₅]²⁻, (dmit), Fig. 1, has been extensively studied as a ligand with both transition and main group metal complexes [1] and binds to metal centres primarily through the thiolato sulfur atoms forming, in the majority of cases, chelate complexes. Intermolecular or interanionic secondary metal–sulfur interactions can also occur to link the neutral or ionic complexes into aggregated species. Such is the case with bis(1,3-dithiole-2-thione-4,5-dithiolato)antimonate(1-) [Q][Sb(dmit)₂], (1) [2,3], and also bis(1,3-dithiole-2-thione-4,5-dithiolato)bismuthate(1-) complexes, [Q][Bi(dmit)₂], (2) [4–6] (Q = quaternary ammonium, arsonium cation, etc). The secondary metal–sulfur bonding in [1: Q = NEt₄, 1,4-

dimethylpyridinium (DMP), or PPh₄] involves the thione sulfur atoms, which connect the bis chelated anions into arrays, varying in form with the cation [Q]⁺. Metal-thione intermolecular interactions also arise in [NBu₄][Bi(dmit)₂] (2: Q = NBu₄) [4], but in (2: Q = NEt₄) [5], [(2: Q = NEt₄)·1/2Et₂O] [5] and [(2: Q = AsPh₄)·1/2DMSO] [4], it is the thiolato sulfur atoms which take part in the secondary bonding. In addition to these metal–sulfur interactions there can be weak intermolecular S··S contacts at distances less than the sum of the van der Waals radii of 3.60 Å, which further interconnect the anionic assemblies. In contrast, there are no interanion interactions in the benzene-1,2-dithiolato complex [NEt₄][Sb(1,2-S₂C₆H₄)₂] (CSD reference code: HEGCUR) in which the benzene-1,2-dithiolato ligand is merely chelating [7].

Related to the dmit ligand is the 1,3-dithiole-2-one-4,5-dithiolate dianion, [C₃OS₄]²⁻ (termed dmio in this paper, but also known as dmid) [1,8]. The structures of few dmio complexes have been reported [1b]. As

* Corresponding author. Tel.: +44-1224-272-907; fax: +44-1224-272-921

E-mail address: r.a.howie@abdn.ac.uk (R. Alan Howie).

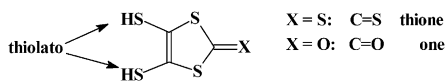


Fig. 1. X = S: H₂dmit; X = O: H₂dmio.

expected, only small structural differences are found between dmit and dmio complexes when these 1,2-dithiolato ligands merely act as chelates, as in [Q][R₂SnX(dmit)] and [Q][R₂SnX(dmio)] [9,10], [Q]₂[Sn(dmit)₃] and [Q]₂[Sn(dmio)₃] [11], as well as [Q][Zn(dmit)₂] and [Q][Zn(dmio)₂] [12]. However, when the chalcogen atoms are involved in secondary bonding, structural differences are realised as is the case with the pair, Me₂Sn(dmit) and Me₂Sn(dmio) [9,13].

A series of bis(1,3-dithiole-2-one-4,5-dithiolato)antimonate(1-) complexes, [Q][Sb(dmio)₂] (**3**) have been prepared and the structures of two complexes, (**3**: Q = NEt₄ and DMP), have been determined and are now reported. These are compared with the structures of the previously reported (**1**: Q = NEt₄, DMP and PPh₄) as well as with those of the new compounds, (**1**: Q = NBu₄ and AsPh₄).

2. Experimental

2.1. General

NMR spectra were run on Bruker 250 and 300 MHz instruments, IR spectra on Nicolet Magna 760 FTIR, Philips Analytical PU9800 and Nicolet Fourier-transform spectrometers and UV–Vis spectra on a Varian–Cary 1E UV–Vis instrument. Melting points (m.p.) were measured on a Melt–TempII instrument and a Kofler hotstage and are uncorrected. Elemental analyses were obtained using a Perkin–Elmer 2400 Instrument or from Butterworth Laboratories Ltd, Middlesex. The compounds, (ferrocenylmethyl)trimethylammonium iodide, [FcCH₂NMe₃]I [14], [Q]₂[Zn(dmit)₂] (Q = NBu₄ and AsPh₄) and [Q]₂[Zn(dmio)₂] (Q = NEt₄, DMP, FcCH₂NMe₃ and PPh₄) [12,15] were prepared by published procedures.

2.1.1. Synthesis of **1** and **3**

These were prepared by a procedure similar to that previously used for (**1**: Q = NEt₄, PPh₄ or DMP) [2,3]. Reactions between SbBr₃–NaSCN and [Q]₂[Zn(dmit)₂] or [Q]₂[Zn(dmio)₂] gave the target products in yields generally greater than 60% after recrystallisation. The procedure used for (**1**: Q = AsPh₄) is given as an illustration.

2.1.2. Compound (**1**: Q = AsPh₄) from [AsPh₄]₂[Zn(dmit)₂]

To a solution of NaSCN·2H₂O (0.351 g, 3 mmol) in acetone (20 cm³) was successively added a solution of

SbBr₃ (0.36 g, 1 mmol) in acetone (20 cm³) and a solution of [AsPh₄]₂[Zn(dmit)₂] (1.22 g, 1 mmol) in acetone (35 cm³). The reaction mixture was stirred for 30 min after the addition of [AsPh₄]₂[Zn(dmit)₂], the solvent removed by rotary evaporation and the crude product recrystallised from acetone to give dark green–black crystals (blocks), m.p. 185–187 °C. *Anal.* for (**1**: Q = AsPh₄). Found: C, 40.2; H, 2.3. C₃₀H₂₀AsS₁₀Sb requires C, 40.1; H, 2.2%. ¹H NMR (DMSO-*d*₆, 300 MHz): δ: 7.8–7.9(m, aryl-H). ¹³C NMR (DMSO-*d*₆, 75.5 MHz): δ: 121.5, 131.5, 133.7 and 134.9(aryl-C), 132.7(C=C), 212.2(C=S). IR (KBr, cm⁻¹): 1437 (C=C), 1053, 1014(C=S), 883(C–S). IR (CsI, cm⁻¹): 516, 482, 463, 398, 360, 351, 323, 289, 279, 270, 246, 223.

2.1.3. Compound (**1**: Q = NBu₄) from [NBu₄]₂[Zn(dmit)₂]

The product was recrystallised from DMSO as dark red crystals (needles): m.p. 168–170 °C. *Anal.* for (**1**: Q = NBu₄). Found: C, 34.8; H, 4.9; N, 1.8. C₂₂H₃₆NS₁₀Sb requires C, 34.9; H, 4.8; N, 1.9%. ¹H NMR (DMSO-*d*₆, 300 MHz): δ: 0.93(t, 12H, *J*(¹H–¹H) = 7.2 Hz, CH₃), 1.30(m, 8H, CH₂), 1.57(m, 8H, CH₂), 3.18(t, 8H, H₂C–N). ¹³C NMR (DMSO-*d*₆, 75.5 MHz): δ: 13.5(CH₃), 19.2(CH₂), 23.1(CH₂), 57.6(CH₂), 132.4(C=C) and 211.5(C=S). IR (KBr, cm⁻¹): 1437(C=C), 1063, 1016(C=S), 889(C–S). IR (CsI, cm⁻¹): 526, 519, 462, 441, 390, 343, 329, 300, 288, 266, 246, 219.

2.1.4. Compound (**3**: Q = NEt₄) from [NEt₄]₂[Zn(dmio)₂]

The target product was recrystallised from acetone as a dark green–black crystalline solid, m.p. 193–195 °C. Yield: 0.57 g (67%). *Anal.* for (**3**: Q = NEt₄). Found: C, 27.6; H, 3.5. C₁₄H₂₀NO₂Sb requires C, 27.5; H, 3.3%. ¹H NMR (DMSO-*d*₆, 250 MHz): δ: 1.2 (t of t, 12H, *J*(¹H–¹H) = 7.2 Hz, Me of cation), 3.2 (q, 8H, *J*(¹H–¹H) = 7.5 Hz, CH₂N of cation). ¹³C NMR (DMSO-*d*₆, 63 MHz): δ: 8.7(Me), 53.0(CH₂N), 119.9(C=C), 195.4(C=O). IR (CsI, cm⁻¹): 2075, 1660, 1607, 1473, 1391, 1365, 1171, 1000, 883, 786, 755, 545, 462, 365, 338, 321, 280, 257, 172.

2.1.5. Compound (**3**: Q = DMP) from [DMP]₂[Zn(dmio)₂]

The target product was recrystallised from acetone as a dark green–black crystalline solid, m.p. 182–183 °C. Yield: 0.58 g (68%). *Anal.* for (**3**: Q = DMP). Found: C, 26.7; H, 1.7; N, 2.5. C₁₃H₁₀NO₂S₈Sb requires C, 26.4; H, 1.7; N, 2.4%. ¹H NMR (DMSO-*d*₆, 250 MHz): δ: 2.6 (s, 3H, Me of cation), 4.3 (s, 3H, MeN of cation), 7.9 (d, 2H, *J*(¹H–¹H) = 6.2 Hz, C₃ and C₅), 8.8 (d, 2H, *J*(¹H–¹H) = 6.6 Hz, C₂ and C₆). ¹³C NMR (DMSO-*d*₆, 63 MHz): δ: 23.1(Me), 48.8(MeN), 120.0(C=C), 129.7, 146.2, 159.9 (aromatic-C), 195.4(C=O). IR (CsI,

cm^{-1}): 1771, 1660, 1641, 1605, 1517, 1471, 1295, 1189, 885, 877, 816, 803, 752, 695, 542, 486, 460, 366, 333, 318, 279, 252, 174, 154.

2.1.6. Compound (3: Q = Ph₄P) from [PPh₄]₂[Zn(dmio)₂]

The target molecule was recrystallised from acetone as a black crystalline solid, m.p. 173–175 °C. Yield: 0.88 g (66%). *Anal.* for (3: Q = Ph₄P). Found: C, 43.5; H, 2.6. C₃₀H₂₀O₂PS₈Sb: requires C, 43.8; H, 2.4%. ¹H NMR (DMSO-*d*₆, 250 MHz): δ : 7.8 (m, 12H, *m*-H + *p*-H), 8.0 (m, 8H, *o*-H). ¹³C NMR (DMSO-*d*₆, 63 MHz): δ : 118.6 (C=C), 120.0 ($J(^{31}\text{P}-^{13}\text{C}) = 88.5$ Hz, C_i), 132.0 [$J(^{31}\text{P}-^{13}\text{C}) = 12.2$ Hz, C_m], 136.1 ($J(^{31}\text{P}-^{13}\text{C}) = 11.0$ Hz, C_o), 137.0 ($J(^{31}\text{P}-^{13}\text{C}) = 2.2$ Hz, C_p), 195.3 (C=O). IR (KBr, cm^{-1}): 1660, 1610, 1585, 1471, 1434, 1104, 995, 885, 752, 686, 526, 460.

2.1.7. Compound (3: Q = FcCH₂NMe₃) from [FcCH₂NMe₃]₂[Zn(dmio)₂]

The target molecule was recrystallised from acetone as a dark orange–green solid, m.p. 203–205 °C. Yield: 0.78 g, (60%). *Anal.* for (3: Q = FcCH₂NMe₃): C, 32.0; H, 3.0; N, 1.7. C₂₀H₂₀NO₂FeS₈Sb requires C, 32.4; H, 2.7; N, 2.0%. ¹H NMR (DMSO-*d*₆, 250 MHz): δ : 2.9 (s, 9H, Me of cation), 4.2 (s, 5H, unsubstituted *cp*-H), 4.4 (s, 4H, substituted *cp*-H), 4.5 (s, 2H, CH₂N). ¹³C NMR (DMSO-*d*₆, 63 MHz): δ : 53.0 (Me), 67.1 (CH₂N), 70.6 (unsubstituted *cp*-C), 71.7, 73.6, 74.7 (substituted *cp*-C), 119.9 (C=C), 195.3 (C=O). IR (KBr, cm^{-1}): 1666, 1610, 1479, 1467, 867, 825, 482, 464.

2.2. Crystallography

2.2.1. Data collection

For (3: Q = NEt₄ or DMP) unit cell and intensity data were obtained at 293 and 150 K, respectively, on the Delft Instruments FAST diffractometer of the EPSRC's crystallographic service at Cardiff. Unit cells were determined and the data collected using the routines ENDEX, REFINE and MADONL of the MADNES software [16] and data reduction carried out using ABSMAD [17]. Full procedural details are available elsewhere [18]. The triclinic cell determined initially for (3: Q = NEt₄) was found to correspond to a C-centred monoclinic cell and the cell dimensions were adjusted accordingly and the intensity data re-indexed with the row-wise transformation matrix $-1 \ -1 \ 0; \ -1 \ 1 \ 0; \ 0 \ 0 \ -1$. In both cases correction for absorption was made using XABS-2 [19].

Unit cell and intensity data for (1: Q = NBu₄) and (1: Q = AsPh₄), both at 150 K, were obtained by means of the Enraf Nonius KappaCCD area detector diffractometer of the EPSRC's crystallographic service at Southampton. The entire process of data collection, cell refinement and data reduction was accomplished by

means of the programs DENZO [20] and COLLECT [21]. Correction for absorption was by means of SORTAV [22].

2.2.2. Structure solution and refinement

The direct methods approach of SHELXS-97 [23] provided solutions for the structures of (1: Q = NBu₄) and (3: Q = NEt₄ or DMP), while the structure of (1: Q = AsPh₄) was solved by the heavy atom method using SHELXS-86 [23]. Structure refinement in all cases was by means of SHELXL-97 [24]. In the case of (1: Q = AsPh₄) correction for extinction was applied with *k* in the formula: $F_c^* = kF_c[1 + 0.001 \times F_c^2 \lambda^3 / \sin(2\theta)]^{1/4}$ taking the value 0.0035(5). In all four cases, all non-H atoms were refined anisotropically and in the final stages H atoms were introduced in calculated positions and refined with a riding model. Special action was required to deal with disorder in two of the Bu groups of the counter cation of (1: Q = NBu₄) and the centrosymmetric symmetry of the cation sites in (3: Q = NEt₄) and (3: Q = DMP). Further details of data collection and structure refinement are available in Table 1.

3. Results and discussion

3.1. General

The dmit complexes, (1: Q = NBu₄ and AsPh₄), were prepared from [Q]₂[Zn(dmit)₂] and SbBr₃–NaSCN in acetone, using a previously reported procedure [2]. A related procedure was used to obtain (3: Q = NEt₄, DMP, PPh₄ or FcCH₂NMe₃) from [Q]₂[Zn(dmio)₂] and SbBr₃–NaSCN. The complexes have little solubility in non-coordinating solvents: the NMR spectra were run in DMSO-*d*₆ for this reason. The values of $\nu(\text{C}=\text{C})$ for 1 and 3 are generally found in the regions 1430–1443 and 1455–1470 cm^{-1} , respectively, while the $\delta^{13}\text{C}(\text{C}=\text{C})$ NMR values are between 132.4–133.9 and 118.6–120.0 ppm, respectively. Spectral data for the C=S groups in 1 $\nu(\text{C}=\text{S})$ 1016–1026 cm^{-1} and $\delta^{13}\text{C}(\text{C}=\text{S})$ 211.5–213.3 ppm: values for C=O in 3 are $\nu(\text{C}=\text{O})$ 1660–1667 and 1605–1610 cm^{-1} and $\delta^{13}\text{C}(\text{C}=\text{O})$ 195.3–195.4 ppm.

3.2. Crystal structures

In what follows, the geometry of the previously published structures of (1: Q = NEt₄, DMP or PPh₄) [2,3] is described in terms of values obtained by the use of PLATON [25] applied to cif data extracted from the Cambridge Structural Database [26] at the Chemical Database Service of the EPSRC at Daresbury [27] with the atomic coordinates unchanged but with the atoms relabelled for conformity with the new structures presented here.

Complexes 1 and 3 are, in all cases, ionic species exhibiting only electrostatic cation–anion interactions.

Table 1
Crystal data and structure refinement

	1: Q = AsPh ₄	1: Q = Nbu ₄	3: Q = Net ₄	3: Q = DMP
Empirical formula	C ₃₀ H ₂₀ AsS ₁₀ Sb	C ₂₂ H ₃₆ NS ₁₀ Sb	C ₁₄ H ₂₀ NO ₂ S ₈ Sb	C ₁₃ H ₁₀ NO ₂ S ₈ Sb
<i>M</i>	897.73	756.87	612.54	590.45
Temperature (K)	150(2)	150(2)	293(2)	150(2)
Wavelength (Å)	0.71073	0.71073	0.71073	0.71073
Crystal system	triclinic	monoclinic	monoclinic	triclinic
Space group	<i>P</i> $\bar{1}$	<i>P</i> 2 ₁ / <i>m</i>	<i>C</i> 2/ <i>c</i>	<i>P</i> $\bar{1}$
Unit cell dimension				
<i>a</i> (Å)	9.1083(1)	9.0802(4)	12.579(7)	8.7965(14)
<i>b</i> (Å)	12.0855(2)	19.1957(8)	12.373(7)	10.741(3)
<i>c</i> (Å)	16.4877(3)	18.0213(10)	14.976(7)	11.251(3)
α (°)	95.6559(6)	90	90	89.310(14)
β (°)	96.1007(6)	94.4590(15)	103.15(3)	100.566(10)
γ (°)	111.0647(13)	90	90	109.903(10)
<i>V</i> (Å ³)	1665.67(4)	3131.6(3)	2270(2)	981.1(4)
<i>Z</i>	2	4	4	2
<i>D</i> _{calc} (g cm ⁻³)	1.790	1.605	1.792	1.999
Absorption coefficient (mm ⁻¹)	2.464	1.563	1.962	2.266
<i>F</i> (000)	888	1544	1224	580
Crystal colour	dark green–black	dark red	dark green–black	dark green–black
Crystal size (mm)	0.36 × 0.20 × 0.06	0.25 × 0.05 × 0.03	0.2 × 0.2 × 0.2	0.22 × 0.14 × 0.07
θ Range for data collection (°)	3.21–30.54	3.09–27.51	2.34–25.02	1.84–25.52
Index range	–11 ≤ <i>h</i> ≤ 11, –15 ≤ <i>k</i> ≤ 17, –21 ≤ <i>l</i> ≤ 23	–11 ≤ <i>h</i> ≤ 11, –24 ≤ <i>k</i> ≤ 24, –21 ≤ <i>l</i> ≤ 23	–14 ≤ <i>h</i> ≤ 14, –9 ≤ <i>k</i> ≤ 13, –16 ≤ <i>l</i> < 11	–10 ≤ <i>h</i> ≤ 9, –12 ≤ <i>k</i> ≤ 12, 0 ≤ <i>l</i> ≤ 11
Reflections collected/unique [<i>R</i> _{int}]	25 181/8684 [0.0390]	19 918/7137 [0.1185]	42 591/1692 [0.0822]	37 532/2752 [0.1443]
Completeness to 2 θ limit (%)	85.2	98.9	84.1	75.2
Absorption correction	semi-empirical from equivalents	semi-empirical from equivalents	empirical (XABS-2.0)	empirical (XABS-2.0)
Max/min transmission	0.864, 0.756	0.959, 0.905	0.641, 0.623	1.000, 0.582
Refinement method	full-matrix least-squares on <i>F</i> ²	full-matrix least-squares on <i>F</i> ²	full-matrix least-squares on <i>F</i> ²	full-matrix least-squares on <i>F</i> ²
Data/restraints/parameters	8684/0/380	7137/0/331	1692/0/138	2752/0/226
Goodness-of-fit on <i>F</i> ²	1.060	0.890	1.065	1.166
Final <i>R</i> indices [<i>I</i> > 2 σ (<i>I</i>)] <i>R</i> ₁	0.0366	0.0522	0.0526	0.0712
<i>wR</i> ₂	0.0876	0.0782	0.1235	0.1881
<i>R</i> indices (all data) <i>R</i> ₁	0.0454	0.1647	0.0591	0.0761
<i>WR</i> ₂	0.0922	0.1018	0.1251	0.1898
Extinction coefficient	0.0035(5)			
Largest difference in peak and hole (e Å ⁻³)	1.061 and –2.020	0.981 and –0.757	2.733 and –0.604	2.696 and –1.210

The cations have their usual geometries and are not discussed further. The V-shape (Table 2) of the anions in **1** and **3** is shown, along with the numbering scheme used, in Fig. 2. The bond lengths and angles within dmit, in **1**, and dmio, in **3**, vary little from complex to complex. The central C=C bond of each of the ligands and its attached S constitutes a planar entity with Sb and the C=O or C=S atoms displaced from this plane by varying amounts as shown in Table 2. In all complexes each of the two chelating dmit–dmio ligands is asymmetrically bound to Sb (Table 3) with shorter and longer Sb–S bond lengths in the range 2.4679(18)–2.527(3) and 2.529(3)–2.7311(6) Å, respectively, both of which can be compared with the PLATON [25] estimate of the sum of the covalent radii of Sb and S of 2.48 Å. As indicated in

the Introduction, the complex, [NET₄][Sb(1,2-S₂C₆H₄)₂], has been reported [7] to have non-interacting anions and have a pseudo 5-coordinate Sb centre, if one coordination site is assumed to be occupied by the antimony lone pair. The dithiolato ligands in [NET₄][Sb(1,2-S₂C₆H₄)₂] [7] are also asymmetrically bonded to Sb, with Sb–S bond lengths of 2.4400(7) and 2.6093(7), in one chelate, and 2.4450(7) and 2.6266(8) Å, in the other and are, therefore, comparable with those in **1** and **3**.

In all of the complexes **1** and **3** antimony also forms two weaker bonds to chalcogen atoms of neighbouring anions with Sb–S and Sb–O, in the range 3.271(4)–3.4968(16) and 3.131(5)–3.285(3) Å respectively (cf. PLATON [25] estimates of sums of van der Waals radii for Sb and S and Sb and O and of covalent radii of Sb

Table 2
Out of plane displacements^a and interplanar and anion V-shape angles, Ip and V (Å, °)

	Sb-oop(Å): Sb out of the ligand plane	C3-oop(Å): C3 out of the ligand plane	X-oop(Å): thione-S or one-O out of the ligand plane	Ip (°): angle between the ligand planes	V (°): angle subtended at Sb by the two thione S in (1) or two one-O in (3)
(1: Q = NEt ₄) ^b	0.247(2)	0.095(11)	0.292(4)	86.52(12)	105.85(11)
(3: Q = NEt ₄)	-0.188(3)	0.054(7)	0.100(6)	86.95(5)	107.42(10)
(1: Q = PPh ₄) ^c	-0.096(1), 1.315(1)	-0.003(5), 0.004(5)	0.003(1), -0.022(2)	67.29(6)	84.5(2)
(1: Q = AsPh ₄)	-0.0819(10), -1.338(9)	0.005(3), 0.004(5)	0.0010(12), 0.0386(14)	66.43(2)	83.39(1)
(1: Q = NBu ₄)	-0.099(2), 1.208(2)	0.031(5), 0.026(6)	0.103(3), 0.216(3)	63.35(5)	82.50(2)
(1: Q = DMP) ^b	0.606(1), 0.141(1)	0.047(10), -0.009(9)	0.091(3), -0.025(3)	66.31(11)	120.8(2)
(3: Q = DMP)	0.030(4), 0.711(4)	-0.030(10), -0.087(15)	0.024(9), -0.158(12)	76.41(9)	97.21(11)

^a Dmit and dmio ligand planes are defined by the C–C double bond and the attached S atoms.

^b Ref. [2].

^c Ref. [3].

and O of 4.06, 3.78 and 2.14 Å, respectively). These link the anions into 2D sheets or chains and in some cases, along with S··S or S··O contacts shorter than the sum of van der Waals radii (3.60 or 3.32 Å, respectively), into 3D networks in a manner described in more detail below.

In all of the structures discussed here, the anions are confined to layers whose orientation is indicated compound by compound in Table 3 and which are stacked alternating with parallel layers of counter cations. The simplest case, the anion layer in isostructural (1 and 3: Q = NEt₄), is clearly evident in Fig. 3(a). Here the disposition of the anions is entirely due to the C-centred nature of the unit cell so that all the anions within a single layer at $z = 1/4$ or $3/4$ point in the same direction along b . Adjacent anion layers are then related to one another by crystallographic centres of symmetry or equivalently by the operation of the c -glide of the space group $C2/c$, thus inverting the orientation of the anions from one layer to the next. Contacts between anion layers as S3··S5ⁱ (i: $1/2-x, 1/2-y, -z$) at 3.556(5) Å in (1: Q = NEt₄) and S3··S1ⁱ (i: $-x, -y, 1-z$) and S3··O1ⁱⁱ (ii: $-1/2-x, -1/2-y, 1-z$) at 3.550(3) and

3.317(5) Å, respectively, in (3: Q = NEt₄) complete the connectivity.

In all of the other compounds discussed in this paper the secondary Sb–S and Sb–O bonds interconnect the anions to form chains. This is brought about in two stages leading to three different situations (Fig. 3(b–d), Tables 3 and 4). In the first stage one atom, X' in Table 3, i.e. a symmetry related equivalent of thione S5 in (1: Q = NBu₄, AsPh₄, PPh₄ and DMP) or of thiolato S2 in (3: Q = DMP), bonds to Sb to form a centrosymmetric dimer in which inevitably a pair of parallel and head to tail ligands overlap to a greater or lesser extent (ring pairs a–a' in Table 4). The second stage involves further contacts, Sb–X'' where X'' (Table 3) is a second and different symmetry related equivalent, relative to the original Sb, of the same thione S5 as before for (1: Q = NBu₄, AsPh₄ and PPh₄), or symmetry equivalent thione S, S10, or one-O, O1, in (1: Q = DMP) [2] or (3: Q = DMP), respectively. These connect the anions in (1: Q = NBu₄, AsPh₄ and PPh₄) (Fig. 3(b)) and (3: Q = DMP) (Fig. 3(c)), to form linear double chains in which the face to face ligands, including their chelate function, are now μ^3 bridging species while the other ligands, protruding on either side of the spine of the double

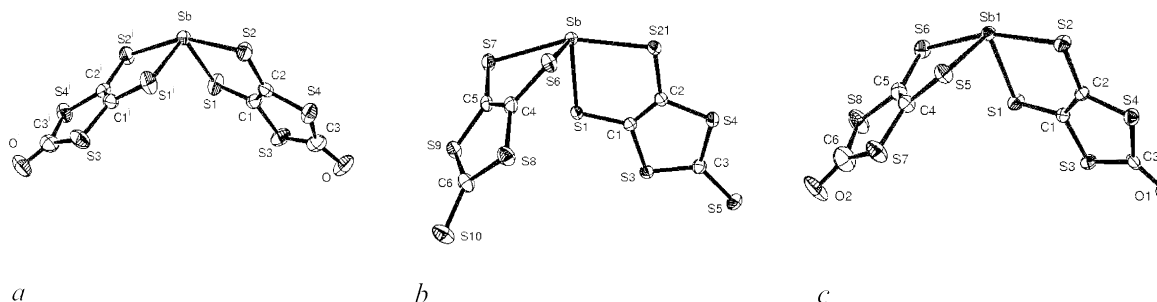


Fig. 2. Atom arrangements and numbering systems for (a) (3: Q = NEt₄) which, with S5 replacing O, applies equally well to (1: Q = NEt₄) [2] as relabelled for comparison purposes; (b) (1: Q = AsPh₄, NBu₄ and relabelled PPh₄ [3] and DMP [2]), AsPh₄ salt shown; (c) (3: Q = DMP).

Table 3
Bond lengths and angles ^a (Å, °) about Sb in anions of **1** and **3**

	(1 :Q = NEt ₄) ^b	(3 :Q = NEt ₄)	(1 :Q = NBu ₄)	(1 :Q = AsPh ₄)	(1 :Q = PPh ₄) ^c	(1 :Q = DMP) ^b	(3 :Q = DMP)
S(A)	S1	S1	S1	S1	S1	S1	S1
S(B)	S2	S2	S2	S2	S2	S2	S2
S(C)	S1' [i]	S1' [i]	S6	S6	S6	S6	S5
S(D)	S2' [i]	S2' [i]	S7	S7	S7	S7	S6
X''	S5' [iii]	O1' [iv]	S5' [vi]	S5' [vi]	S5' [ix]	S10' [xi]	O1' [vi]
X'	S5'' [iii]	O1'' [v]	S5'' [vii]	S5'' [viii]	S5'' [x]	S5' [xii]	S2' [viii]
<i>Bond lengths</i>							
Sb–S(A)	2.496(3)	2.4679(18)	2.4883(15)	2.4825(6)	2.4777(12)	2.502(3)	2.527(3)
Sb–S(B)	2.673(3)	2.666(2)	2.6047(15)	2.6146(6)	2.6194(13)	2.696(3)	2.648(3)
Sb–S(C)	2.496(3)	2.4679(18)	2.4854(16)	2.5114(6)	2.5080(15)	2.527(3)	2.478(3)
Sb–S(D)	2.673(3)	2.666(2)	2.7228(16)	2.7311(6)	2.7235(16)	2.661(3)	2.529(3)
Sb–X'	3.271(4)	3.131(5)	3.4968(16)	3.3721(7)	3.4016(17)	3.336(4)	3.285(3)
Sb–X''	3.271(4)	3.131(5)	3.3413(15)	3.4965(7)	3.5495(15)	3.354(4)	3.173(8)
Sb...Sb'	–	–	4.3098(8)	4.0636(3)	4.0785(10)	–	3.6008(15)
<i>Bond angles</i>							
S(A)–Sb–S(B)	83.22(13)	83.12(6)	84.45(5)	84.08(2)	84.1(2)	82.6(2)	83.70(8)
S(C)–Sb–S(D)	83.22(13)	83.12(6)	80.55(5)	80.34(2)	80.3(2)	82.9(2)	83.42(9)
S(A)–Sb–S(C)	101.65(13)	105.26(10)	97.17(6)	95.73(2)	95.7(2)	101.5(2)	96.52(9)
S(B)–Sb–S(D)	158.86(13)	157.47(18)	158.99(5)	158.72(2)	159.5(2)	155.6(2)	162.81(9)
S(A)–Sb–S(D)	83.47(13)	83.27(6)	77.97(5)	76.347(19)	77.2(2)	81.3(2)	82.54(9)
S(B)–Sb–S(C)	83.47(13)	83.27(6)	90.43(5)	93.61(2)	93.5(2)	82.5(2)	87.97(9)
X'–Sb–X''	103.54(13)	100.6(2)	101.90(3)	107.481(14)	108.2(2)	103.4(2)	115.84(15)
X'–Sb–S(A)	82.44(13)	86.16(10)	83.40(4)	83.837(18)	83.2(2)	86.1(2)	82.32(8)
X'–Sb–S(B)	120.55(13)	128.96(11)	78.25(4)	85.946(18)	86.8(2)	123.2(2)	106.15(7)
X'–Sb–S(C)	155.98(13)	147.36(10)	168.58(5)	179.409(19)	178.9(2)	154.1(2)	165.56(8)
X'–Sb–S(D)	73.67(13)	67.71(12)	110.64(3)	99.935(18)	99.1(2)	73.8(2)	82.15(8)
X''–Sb–S(A)	155.98(13)	147.36(10)	148.45(4)	145.204(18)	145.8(2)	156.5(2)	151.94(15)
X''–Sb–S(B)	73.67(13)	67.71(12)	66.67(4)	64.661(17)	65.1(2)	74.2(2)	71.06(14)
X''–Sb–S(C)	82.44(13)	86.16(10)	71.73(5)	72.656(18)	72.9(2)	79.4(2)	71.15(15)
X''–Sb–S(D)	120.55(13)	128.96(11)	126.70(4)	130.899(18)	129.8(2)	121.8(2)	119.47(14)
Direction of chain propagation ^d			<i>a</i>	<i>a</i>	<i>c</i>	<i>a</i>	<i>a</i>
Orientation of chain ^e	(001)	(001)	(010)	(010)	(100)	(011)	(011)

For all but (**1**: Q = NEt₄) and (**3**: Q = NEt₄), X'' is the atom which connects the anions into chains, and X' is the atom used to connect the anions in centrosymmetric pairs with face to face ligands.

^a Symmetry operations as designated by roman numerals in square brackets: i: $-x, y, 1/2-z$; ii: $x-1/2, 1/2+y, z$; iii: $1/2-x, 1/2+y, 1/2-z$; iv: $-1/2-x, 1/2+y, 1/2-z$; v: $1/2+x, 1/2+y, z$; vi: $x-1, y, z$; vii: $1-x, 1-y, 1-z$; viii: $1-x, 1-y, -z$; ix: $x, y, z-1$; x: $1-x, -y, 1-z$; xi: $1-x, y, z$; xii: $1-x, 2-y, 2-z$.

^b Ref. [2].

^c Ref [3].

^d Direction of propagation of anion chains.

^e Form of plane parallel to anion (and cation) layers.

chain, are purely chelating. In (**1**: Q = DMP) [2], on the other hand, the secondary Sb–S10 bond, which was overlooked in the original report of this structure, creates a chain in the form of a succession of loops, Fig. 3(d), and both ligands are now μ^2 bridges while still chelating.

In the case of (**1**: Q = AsPh₄) and (**1**: Q = PPh₄) [3], which are isostructural despite the different labelling of the cell edges, there is no significant contact between the linear chains within or between the layers and adjacent layers being related to one another purely by cell translation are all identical. In (**1**: Q = NBu₄), which is isostructural with (**2**: Q = NBu₄) [4], there is likewise no

significant contact between the chains but adjacent anion layers are now related by the operation of the *n*-glide of the space group *P2₁/n*. In (**1**: Q = DMP) [2], there is no significant contact between the anion layers, once again related by cell translation and, therefore, all identical, where the looped chains are opposed face to face but within the layers edge to edge contacts between the chains as S5'...S5_i (*i*: $1-x, 3-y, 2-z$) and S5'...S9ⁱⁱ (*ii*: $1+x, 1+y, z$) at 3.387(4) and 3.544(4)Å, respectively, are found (Fig. 3(d)). Also present here between the chains within the layer is limited overlap of centrosymmetrically related pairs of loop forming ligands comprising C4–C6 and S6–S10 (ring pair b–b'

Table 4

Ring overlaps in terms of PLATON [25] π – π interaction parameters (\AA , $^\circ$) and lateral displacements, O

	Ring pair ^a [symmetry operation]	<i>A</i>	α	β	β'	<i>B</i>	<i>B'</i>	O ^b
(1: Q = NBu ₄)	a–a' [vii]	3.534	0	12.80	12.80	3.447	3.447	0.779
(1: Q = AsPh ₄)	a–a' [viii]	3.512	0	13.37	13.37	3.417	3.417	0.811
(1: Q = PPh ₄) ^c	a–a' [x]	3.541	0	13.02	13.02	3.450	3.450	0.798
(1: Q = DMP)	a–a' [xii]	4.245	0	33.50	33.50	3.540	3.540	2.359
	b–b' [xiii]	5.571	0	48.99	48.99	3.654	3.654	4.205
	a–c' [xiv]	3.732	8.88	18.20	24.53	3.395	3.545	1.374
(3: Q = DMP) ^d	a–a' [xv]	4.441	0	32.77	32.77	3.734	3.734	2.404
	d–d' [x]	4.960	0	51.73	51.73	3.072	3.072	3.894
	e–e' [vii]	4.068	0	40.14	40.14	3.110	3.110	2.622

^a Rings defined as: (a) C1, C2, S4, C3, S3; (b) C4, C5, S7, C6, S6; (c) the DMP ring; (d) C4, C5, S8, C6, S7; (e) Sb, S1, C1, C2, S2. Symmetry operations as in Table 3, plus: xiii: $-x, 1-y, 1-z$; xiv: $1-x, 2-y, 1-z$; xv: $2-x, 1-y, -z$.

^b Calculated as $(A^2 - B^2)^{1/2}$ for all except in (1: Q = DMP) for the a–c' overlap, which was calculated as $[A^2 - (B+B')^2/4]^{1/2}$. The overlap of rings *x* and *y* with centroids Cg_{*x*} and Cg_{*y*} and points F_{*x*} (or F_{*y*}) defined as the foot of the perpendicular from Cg_{*x*} (or Cg_{*y*}) to the plane of ring *y* (or *x*) is defined in the manner used by PLATON [25] in terms of the following: distances Cg_{*x*}–Cg_{*y*} (*A*); Cg_{*x*}–F_{*x*} (*B*) and Cg_{*y*}–F_{*y*} (*B'*) and angles between the ring planes (α); Cg_{*y*}–Cg_{*x*}–F_{*x*} (β) and Cg_{*x*}–Cg_{*y*}–F_{*y*} (β'). If the rings are related to one another by the operation of a crystallographic centre of symmetry they are by definition parallel to one another and hence $\alpha = 0$, $\beta = \beta'$ and $B = B'$.

^c Ref. [3].

^d Ref. [2].

in Table 4). More significant is π – π overlap between the DMP counter cation and the dimer forming ligand (ring pair a–c' in Table 4). In (3: Q = DMP) there is yet again no significant contact between chains within or between layers. However, in this case the use of thiolato S2 in dimer formation promotes overlaps d–d' and e–e' (Table 4) within the essentially linear double chains.

3.3. Geometry at Sb

In all of the complexes **1** and **3**, Sb forms six bonds in two groups as four strong intra- and two weaker inter-anion bonds. Inclusion of the Sb lone pair results in pseudo seven-coordinate geometry probably pentagonal bipyramidal in form (see reference [28]). In contrast, the antimony geometry in [NEt₄][Sb(1,2-S₂C₆H₄)₂] is reported to be pseudo trigonal bipyramidal [7]. The site of the lone pair in compounds (1: Q = NBu₄ or AsPh₄) is assumed to be as shown in Fig. 4(b) and is exactly the same, allowing for the changed atom numbering scheme, as that previously reported for (1: Q = PPh₄) [3]. In all three complexes, the lone pairs on centrosymmetrically related Sb atoms are directed away from one another on opposite sides of the centrosymmetric Sb₂S₂ rings and are in equatorial sites between S5' and S7. The S5'–Sb–S7 angles [X''–Sb–S(D) in Table 3] are less than twice the ideal ligand–M–ligand angle of 72° but are perceived as sufficiently large [$>126.70(4)^\circ$] to accommodate the lone pair. The axial atoms are S5'' and S6 with angles at Sb [X'–Sb–S(C)] of 168.58(5)°, 179.409(19)° and 178.9(2)°, respectively.

The situation in (3: Q = DMP) is similar with the lone pair between O1' and S6 (Fig. 4(d)). The angle O1'–Sb–S6 is only 119.47(14)° but still regarded as large enough to accommodate the lone pair. The axial atoms are now

S2' and S5 making an angle of 165.56(8)° at Sb which also shows a greater departure from the ideal than the corresponding angles in the previous cases.

The location of the lone pair in isostructural (1 and 3: Q = NEt₄) is not so simply or obviously determined. In the earlier report on the structure of (1: Q = NEt₄) [2], it was considered to be in an equatorial site between the two Sb–S5 inter-anion bonds, i.e. directed along the crystallographic twofold axis (Fig. 4(a)). It then bisects an angle of only 103.54(13)° which appears extremely small to accommodate it. However, the estimate of this angle has been increased by positing [2] an increase to that of ϕ (Fig. 5), which is achieved if the inter-anion bonds from Sb are directed toward p-orbitals on S (or O) rather than directly toward the atoms. The equivalent bond angle in (3: Q = NEt₄) is still less at 100.6(2)° but the same argument regarding the use of ϕ applies here also. The difference between ϕ and the X–Sb–X bond angle (X = S5 or O1) for the same orbitals increases as the Sb–X bond lengths decrease and the inter-anion bonds Sb–S5 and Sb–O1 are the shortest of all inter-anion bonds found in **1** and **3**. Thus the impact of considering orbital overlap rather than direct atom to atom vectors to determine bond direction and hence bond angles will be greatest for these two complexes. With the lone pairs in equatorial sites directed along the twofold axis as just described the axial sites are then occupied by S2 atoms which form the longest intra-anion bonds in these complexes which is appropriate for their perceived axial status. The angle they form, while only about 158°, is, however, the largest subtended at Sb.

Bearing in mind the twofold axial symmetry of these last two complexes, alternative dispositions of the lone pair can also be envisaged. In (3: Q = NEt₄) the bond

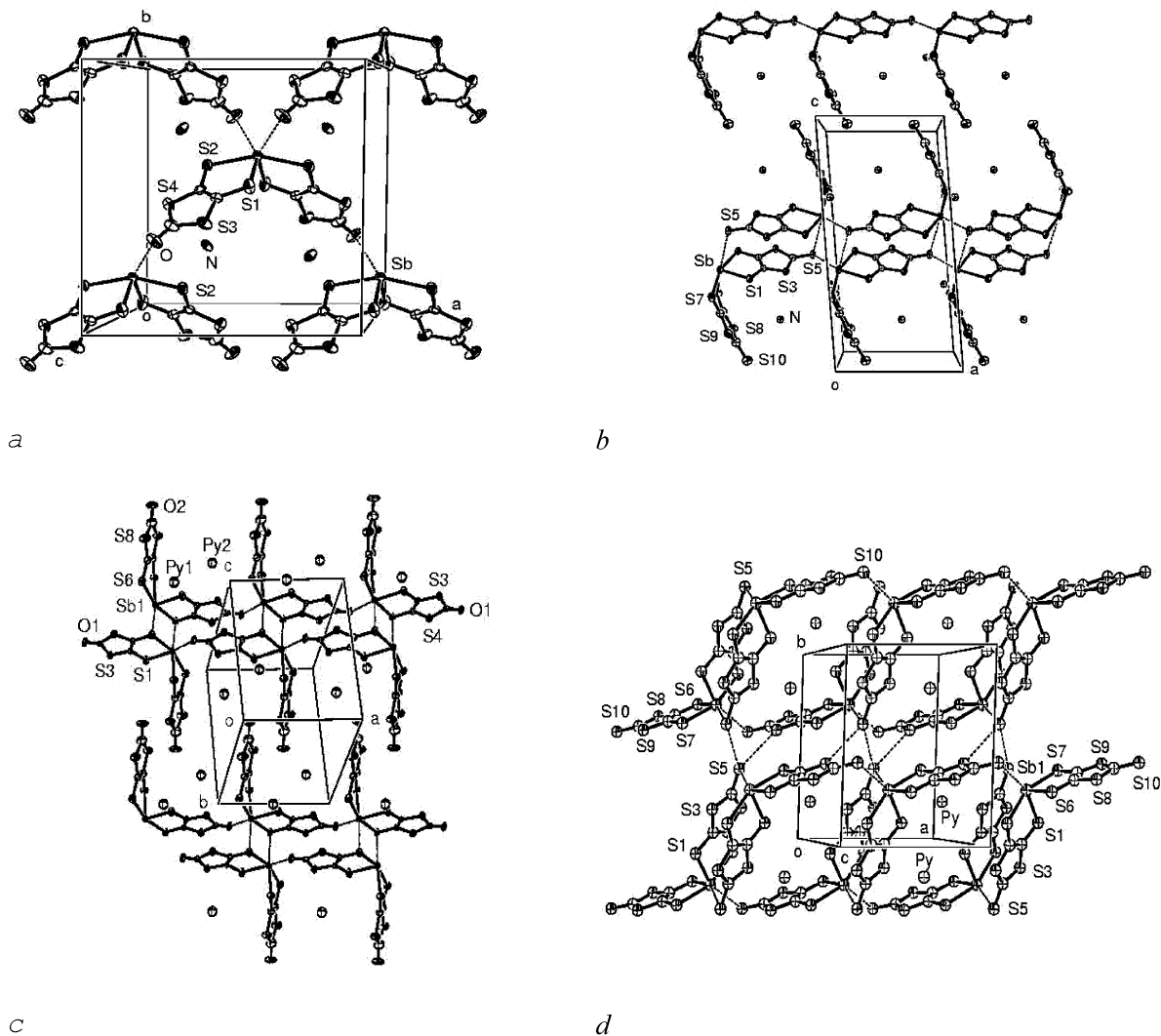


Fig. 3. Anion layers in (a) (**3**: Q = NEt₄), (b) (**1**: Q = NBu₄), (c) (**3**: Q = DMP) and (d) (**1**: Q = DMP) [2]. In all cases only selected atoms are labelled and in a generic manner i.e. lacking symmetry relationships which are instead given in Table 3. Cations are crudely represented either by N or for DMP by the centroid. Atoms are shown as 50% ellipsoids [isotropic atoms for (**1**: Q = DMP)] and the cell edges are labelled. Dashed lines represent Sb–X (X = thione S or one-O) bonds or, in (d), S···S contacts.

angles $O1'-Sb1-S2 = O1''-Sb1-S2' = 128.96(11)^\circ$, associated with axial pairs $O1''-S1$ and $O1'-S1'$ with *trans*-axial angle $147.36(10)^\circ$, are sufficiently large to accommodate the lone pair more easily. If the lone pair occupies only one of these sites the axial symmetry is destroyed but, if the lone pair on Sb occupied an orbital of *d*-type character, it would no longer concentrate electron density towards a single notional coordination site. A similar situation obtains for (**1**: Q = NEt₄) and, see below, (**1**: Q = DMP). Dispersal or smearing out of the lone pair electron density in this way is also consistent with the comparatively short inter-anion Sb–X bonds observed in these complexes.

While crystallographic symmetry does not apply in the case of the remaining complex (**1**: Q = DMP) the

atom pairs S1–S6, S2–S7 and S5'–S10' approximate twofold axial symmetry in their disposition (Fig. 4(c)). On this basis the situation in (**1**: Q = DMP) with angles $S10'-Sb-S5'$ [$103.4(2)^\circ$], $S2-Sb-S7$ [$159.5(2)^\circ$], $S10'-Sb-S7$ [$121.8(2)^\circ$] and $S5'-Sb-S2$ [$123.2(2)^\circ$] relates to that in (**3**: Q = NEt₄) and (**1**: Q = NEt₄) with corresponding angles of similar magnitude.

4. Supplementary material

Crystallographic data for the structural analyses have been deposited with the Cambridge Crystallographic Data Centre, CCDC numbers 174409–174412. Copies of this information may be obtained free of charge from

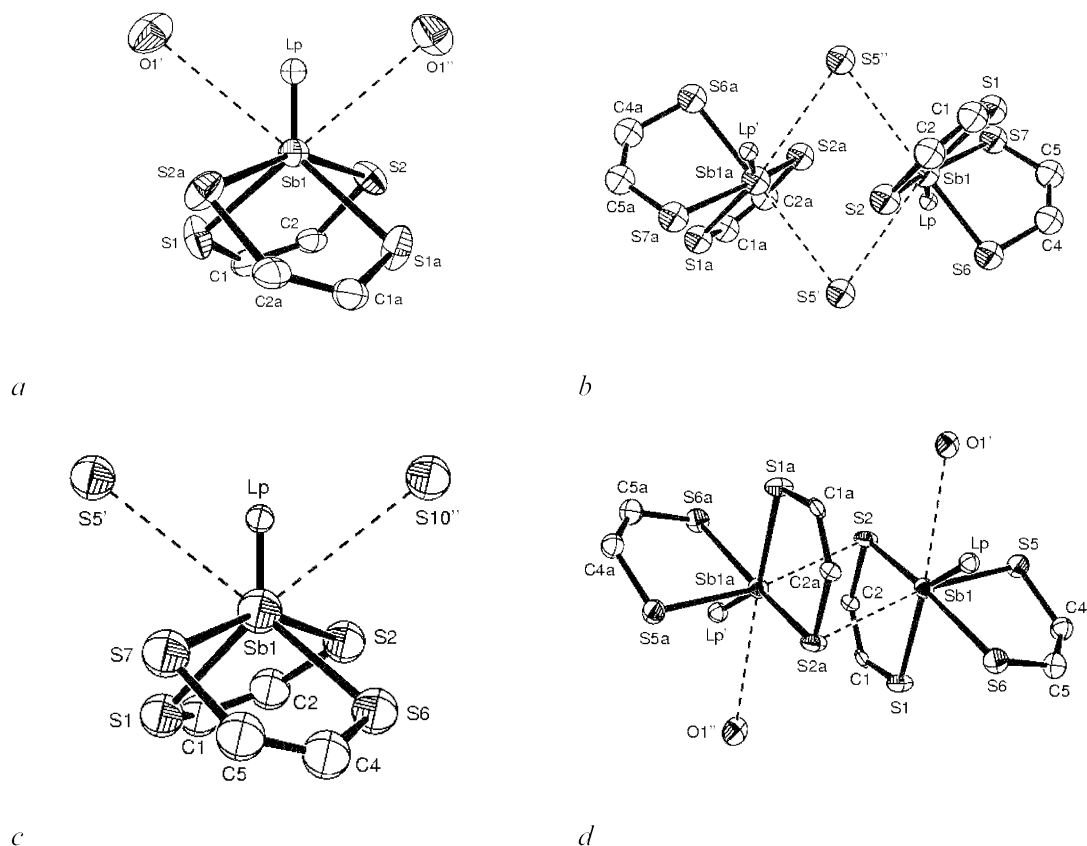


Fig. 4. Representations of the co-ordination of Sb including the stereochemically active lone pair (Lp and where appropriate the centrosymmetrically related Lp') in (a) (1: Q = NEt₄) and (3: Q = NEt₄); (b) (1: Q = NBu₄, PPh₄ or AsPh₄) [the example shown is (1: Q = PPh₄)]; (c) (1: Q = DMP) and (d) (3: Q = DMP). In (a), (b) and (d) the suffix 'a' marks atoms related by symmetry to atoms without suffix. For clarity the ligands providing the primary coordination of Sb are indicated only in terms of the 5-membered chelate rings thus formed.

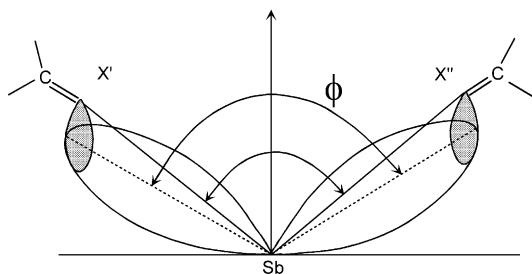


Fig. 5. Comparison of the angle, ϕ , from overlap of Sb and S (or O) orbitals with the S–Sb–S (or O–Sb–O) bond angle.

the Director, CCDC, 12 Union Road, Cambridge CB2 1EZ, UK (fax: +44-1223-336033; e-mail: deposit@ccdc.cam.ac.uk or [www: http://www.ccdc.cam.ac.uk](http://www.ccdc.cam.ac.uk)).

Acknowledgements

We acknowledge the use of the Chemical Database Service of the EPSRC at Daresbury, UK and the

National Data Collection Service of the EPSRC, now at the University of Southampton, previously at the University of Wales, Cardiff, and the expert assistance of the staff there. The financial support of CNPq, FAPERJ and FUJB, Brazil is gratefully acknowledged.

References

- [1] (a) P. Cassoux, *Coord. Chem. Rev.* 186 (1999) 213; (b) A.E. Pullen, R.M. Olk, *Coord. Chem. Rev.* 188 (1999) 211.
- [2] S.M.S.V. Doidge-Harrison, J.T.S. Irvine, G.M. Spencer, J.L. Wardell, P. Ganis, G. Valle, *Inorg. Chem.* 34 (1995) 4581.
- [3] P. Ganis, D. Marton, G.M. Spencer, J.L. Wardell, S.M.S.V. Wardell, *Inorg. Chim. Acta* 308 (2000) 139.
- [4] N.M. Comerlato, W.T.A. Harrison, R.A. Howie, A.C. Silvino, J.L. Wardell, S.M.S.V. Wardell, *Inorg. Chem. Commun.* 3 (2000) 572.
- [5] T. Sheng, X. Wu, P. Lin, W. Zhang, Q. Wang, L. Chen, *Polyhedron* 18 (1999) 1049.
- [6] N.M. Comerlato, L.A.C. Costa, R.A. Howie, R.P. Pereira, A.M. Rocco, A.C. Silvino, J.L. Wardell, S.M.S.V. Wardell, *Polyhedron* 20 (2001) 415.
- [7] J. Wegener, K. Kirschbaum, D.M. Giolando, *J. Chem. Soc., Dalton Trans.* (1994) 1213.
- [8] (a) J.M. Hough, C.A. Haney, R.D. Bereman, C.E. Keefer, *J. Coord. Chem.* 51 (2000) 45;

- (b) H. Müller, A.P. Molina, B.Z. Narymbetov, L.V. Zorina, S.S. Khasanov, R.P. Shibaeva, Z. Anorg. Allg. Chem. 624 (1998) 1492.
- [9] Z.H. Chohan, R.A. Howie, J.L. Wardell, J. Organomet. Chem. 577 (1999) 140.
- [10] (a) J.H. Aupers, Z.H. Chohan, P.J. Cox, S.M.S.V. Doidge-Harrison, R.A. Howie, A. Khan, G.M. Spencer, J.L. Wardell, Polyhedron 17 (1998) 4475;
(b) Z.H. Chohan, J.L. Wardell, J.N. Low, P.R. Meehan, G. Ferguson, Acta Crystallogr. Sect. C 54 (1998) 1401.
- [11] F. de Assis, Z.H. Chohan, R.A. Howie, A. Khan, J.N. Low, G.M. Spencer, J.L. Wardell, S.M.S.V. Wardell, Polyhedron 18 (1999) 3533.
- [12] Z.H. Chohan, R.A. Howie, J.L. Wardell, R. Wilkens, S.M.S.V. Doidge-Harrison, Polyhedron 16 (1997) 2689 (and references therein).
- [13] G.M. Allan, R.A. Howie, J.M.S. Skakle, J.L. Wardell, S.M.S.V. Wardell, J. Organomet. Chem. 627 (2001) 189.
- [14] D. Lednicer, C.R. Hauser, Org. Synth. 40 (1960) 31.
- [15] L. Valade, J.P. Legros, M. Bousseau, P.J. Cassoux, J. Chem. Soc., Dalton Trans. (1985) 783.
- [16] J.W. Pflugrath, A. Messerschmidt, MADNES version 11, September, 1989. Distributed by Delft Instruments, Delft, The Netherlands.
- [17] A.I. Karaulov, ABSMAD. Program for FAST Data Processing, University of Wales, Cardiff, Wales, 1992.
- [18] J.A. Darr, S.R. Drake, M.B. Hursthouse, K.M.A. Malik, Inorg.Chem. 32 (1993) 5704.
- [19] S. Parkin, B. Moezzi, H. Hope, J. Appl. Crystallogr. 28 (1995) 53.
- [20] Z. Otwinowski, W. Minor, Macromolecular crystallography, Part A, in: C.W. Carter, R.M. Sweet (Eds.), Methods in Enzymology, vol. 276, Academic Press, New York, 1997, pp. 307–326.
- [21] R. Hooft, COLLECT, Nonius BV, Delft, The Netherlands, 1998.
- [22] (a) R.H. Blessing, Acta Crystallogr., Sect. A 51 (1995) 33–37;
(b) R.H. Blessing, J. Appl. Crystallogr. 30 (1997) 421.
- [23] G.M. Sheldrick, Acta Crystallogr., Sect. A 46 (1990) 467.
- [24] G.M. Sheldrick, SHELXL-97. Program for Crystal Structure Refinement, University of Göttingen, Germany, 1997.
- [25] A.L. Spek, Acta Crystallogr., Sect. A 46 (1990) c-34.
- [26] F.H. Allen, O. Kennard, Chem. Des. Autom. News (1993) 1 and 31.
- [27] D.A. Fletcher, R.F. McMeeking, D. Parker, J. Chem. Inf. Comput. Sci. 36 (9) (1996) 746.
- [28] (a) R.J. Gillespie, Can. J. Chem. 38 (1960) 818;
(b) J.F. Sawyer, R.J. Gillespie, Prog. Inorg. Chem. 34 (1986) 65.